Suppression of neuropil aggregates and neurological symptoms by an intracellular antibody implicates the cytoplasmic toxicity of mutant huntingtin

Chuan-En Wang,[1] Hui Zhou,[1] John R. McGuire,[1] Vincenzo Cerullo,[2] Brendan Lee,[2,3] Shi-Hua Li,[1] and Xiao-Jiang Li[1]

[1]Department of Human Genetics, Emory University School of Medicine, Atlanta, GA 30322
[2]Department of Molecular and Human Genetics, [3]Howard Hughes Medical Institute, Baylor College of Medicine, Houston, TX 77030

Mutant huntingtin accumulates in the neuronal nuclei and processes, which suggests that its subcellular localization is critical for the pathology of Huntington's disease (HD). However, the contribution of cytoplasmic mutant huntingtin and its aggregates in neuronal processes (neuropil aggregates) has not been rigorously explored. We generated an intracellular antibody (intrabody) whose binding to a unique epitope of human huntingtin is enhanced by polyglutamine expansion. This intrabody decreases the cytotoxicity of mutant huntingtin and its distribution in neuronal processes. When expressed in the striatum of HD mice via adenoviral infection, the intrabody reduces neuropil aggregate formation and ameliorates neurological symptoms. Interaction of the intrabody with mutant huntingtin increases the ubiquitination of cytoplasmic huntingtin and its degradation. These findings suggest that the intrabody reduces the specific neurotoxicity of cytoplasmic mutant huntingtin and its associated neurological symptoms by preventing the accumulation of mutant huntingtin in neuronal processes and promoting its clearance in the cytoplasm.

Introduction

The expansion of a polyglutamine (polyQ) tract in mutant proteins causes Huntington's disease (HD) and eight other known neurodegenerative diseases, including spinocerebellar ataxia and spinobulbar muscular atrophy (Zoghbi and Orr, 2000). The accumulation of expanded polyQ-containing proteins in the nucleus and the subsequent formation of nuclear inclusions are pathological hallmarks of these diseases (Gatchel and Zoghbi 2005; Butler and Bates, 2006). In the majority of polyQ diseases, the mutant proteins carry nuclear localization sequences and are therefore localized primarily in the nucleus. However, huntingtin (htt), a 350-kD protein with a polyQ domain in its N-terminal region, is predominantly localized in the cytoplasm. Generation of polyQ-containing N-terminal htt fragments by proteolysis leads to the accumulation of toxic peptides (Ellerby and Orr, 2006) that also form aggregates in the nucleus and the neuronal processes (neuropil aggregates), which include axons and dendrites (DiFiglia et al., 1997; Gutekunst et al., 1999; Lunkes et al., 2002; Wellington et al., 2002; Graham et al., 2006). Furthermore, polyQ expansion clearly causes protein misfolding and conformational alteration, leading to abnormal protein interactions and transcriptional dysregulation in the nucleus (Zoghbi and Orr, 2000; Sugars and Rubinsztein, 2003; Li and Li, 2004; Butler and Bates, 2006). Notably, the brains of HD patients at the early stage of disease contain more neuropil aggregates than nuclear inclusions (Gutekunst et al., 1999). Also, the progressive formation of neuropil aggregates is correlated with disease progression in transgenic mice (Li et al., 1999, 2000; Schilling et al., 1999; Tallaksen-Greene et al., 2005), and these aggregates are associated with axonal degeneration in HD mouse models (Li et al., 2001; Yu et al., 2003). Given the abundance of neuropil aggregates in HD patient brains, understanding the contribution of cytoplasmic htt to HD pathology is imperative.

Unlike nuclear inclusions, neuropil aggregates have not been studied extensively because of their small size. Although

Correspondence to X.-J. Li: xiaoli@genetics.emory.edu

Abbreviations used in this paper: CMV, cytomegalovirus; HD, Huntington's disease; htt, huntingtin; polyP, polyproline; polyQ, polyglutamine; scFv, single-chain Fv.

The online version of this paper contains supplemental material.

The Rockefeller University Press $30.00
J. Cell Biol. Vol. 181 No. 5 803–816
www.jcb.org/cgi/doi/10.1083/jcb.200710158

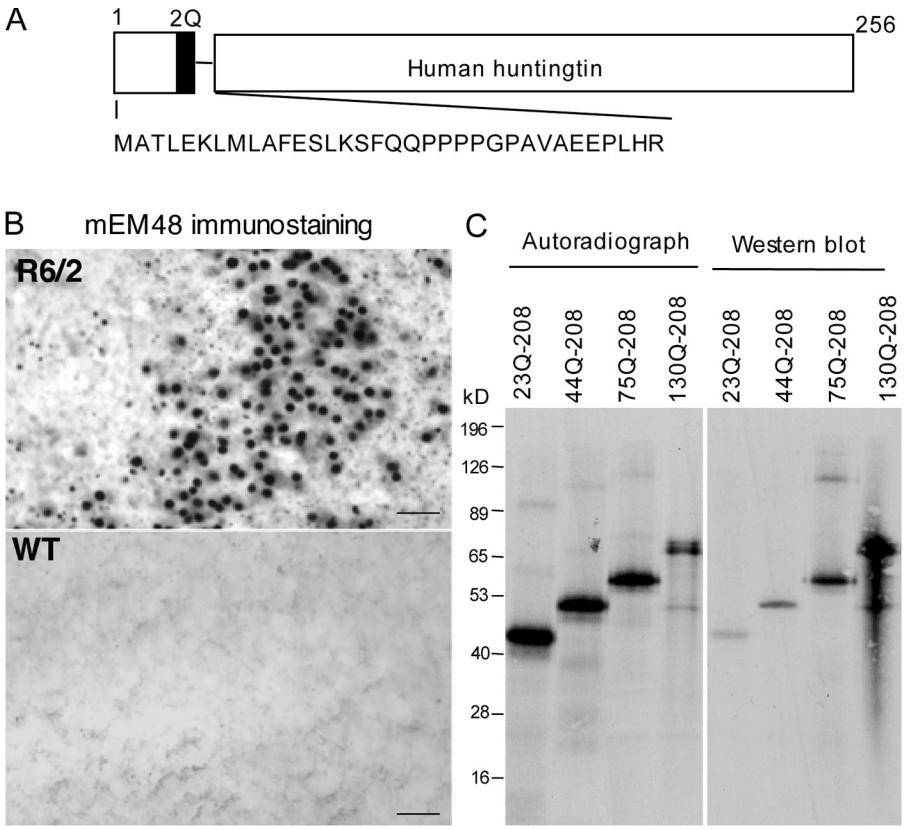

Figure 1. **mEM48 preferentially binds mutant htt.** (A) An N-terminal fragment of human htt used to generate the mouse monoclonal antibody mEM48. The gap represents the missing polyQ and polyP domains in this antigen. The black box indicates two glutamines (2Q). Amino acid numbers are indicated. (B) mEM48 immunostaining of the hippocampal sections from HD transgenic (R6/2) and wild-type (WT) mice at 12 wk of age. Note that the antibody specifically reacts with intranuclear mutant htt aggregates and smaller neuropil aggregates outside the nucleus. Bar, 5 µm. (C) ^{35}S-labeled N-terminal htt (aa 1–208) fragments containing various glutamine repeats (23, 44, 75, and 130Q) were synthesized in vitro, resolved by SDS-PAGE, and revealed by autoradiography (24 h exposure). The same blot was then probed with mEM48 and visualized with ECL reagents (1 min exposure). Note that mEM48 preferentially reacts with N-terminal htt containing longer repeats.

the role of htt aggregates remains controversial (Saudou et al., 1998; Yamamoto et al., 2000; Arrasate et al., 2004; Chang et al., 2006), subcellular localization seems to be critical for the effects of mutant htt and its aggregates. Given the limited confines of neuronal processes, it is conceivable that neuropil aggregates are sizeable enough to physically block intracellular transport. In any case, the formation of neuropil aggregates does reflect the transport and accumulation of toxic htt fragments in neuronal processes and allows us to investigate the toxic effects of cytoplasmic mutant htt in the unique neuronal structure. The normal function of neuronal processes is dependent on the proper transport of proteins and nutrients from the cell body to nerve terminals and may be more vulnerable than nuclear function to a variety of insults. Understanding the effects of cytoplasmic mutant htt in neuronal processes would be useful in the development of an effective treatment strategy for HD patients.

In the present study, we developed an intracellular antibody (intrabody) based on a compelling feature of one unique htt antibody, EM48, which preferentially reacts with mutant htt (Gutekunst et al., 1999; Graham et al., 2006). This intrabody, when expressed in neurons, reduces the cytotoxicity of N-terminal mutant htt and decreases both the formation of neuropil aggregates and the neurological symptoms of HD mice. We further demonstrated that this intrabody promotes the degradation of cytoplasmic mutant htt by increasing its ubiquitination. These findings suggest that the intrabody specifically targets mutant htt with abnormal conformation and can serve as a valuable tool to specifically reduce the cytoplasmic neuropathology of HD.

Results

Generation of an intrabody that preferentially binds mutant htt

Previously, we used a GST fusion protein containing the first 256 amino acids of human htt as the antigen to generate rabbit antibody EM48 (Fig. 1 A). This antigen lacks the polyQ and polyproline (polyP) domains but generates polyclonal EM48 antibodies that selectively label mutant htt (Gutekunst et al., 1999). Using this same antigen, we obtained a mouse monoclonal antibody, mEM48. Although mEM48 also reacts strongly with exon1 mutant htt containing 150Q in R6/2 mouse brain, it does not label normal htt at endogenous levels (Fig. 1 B). Using 1C2, a mouse monoclonal antibody that reacts with expanded polyQ tracts, we also observed similar nuclear and neuropil aggregates in N171-82Q mouse brains (Fig. S1 A, available at http://www.jcb.org/cgi/content/full/jcb.200710158/DC1). Furthermore, mutant htt tagged with the HA epitope at its C terminus formed intracellular aggregates in HEK293 cells, which were recognized by mEM48 and an antibody to the HA epitope (Fig. S1 B). To verify whether this monoclonal antibody binds mutant htt more tightly than normal htt, we used the in vitro synthesis method to generate N-terminal htt fragments (1–208 aa) containing different polyQ domains (23Q, 44Q, 75Q, and 130Q), which were labeled by [^{35}S]methionine. Autoradiography revealed htt fragments with longer polyQ domains synthesized in lesser amounts. The synthesized mutant htt did not show the aggregate form in the gel, perhaps because of the brief time allotted for its synthesis in vitro. Nonetheless, these mutant htt fragments with longer polyQ domains exhibited

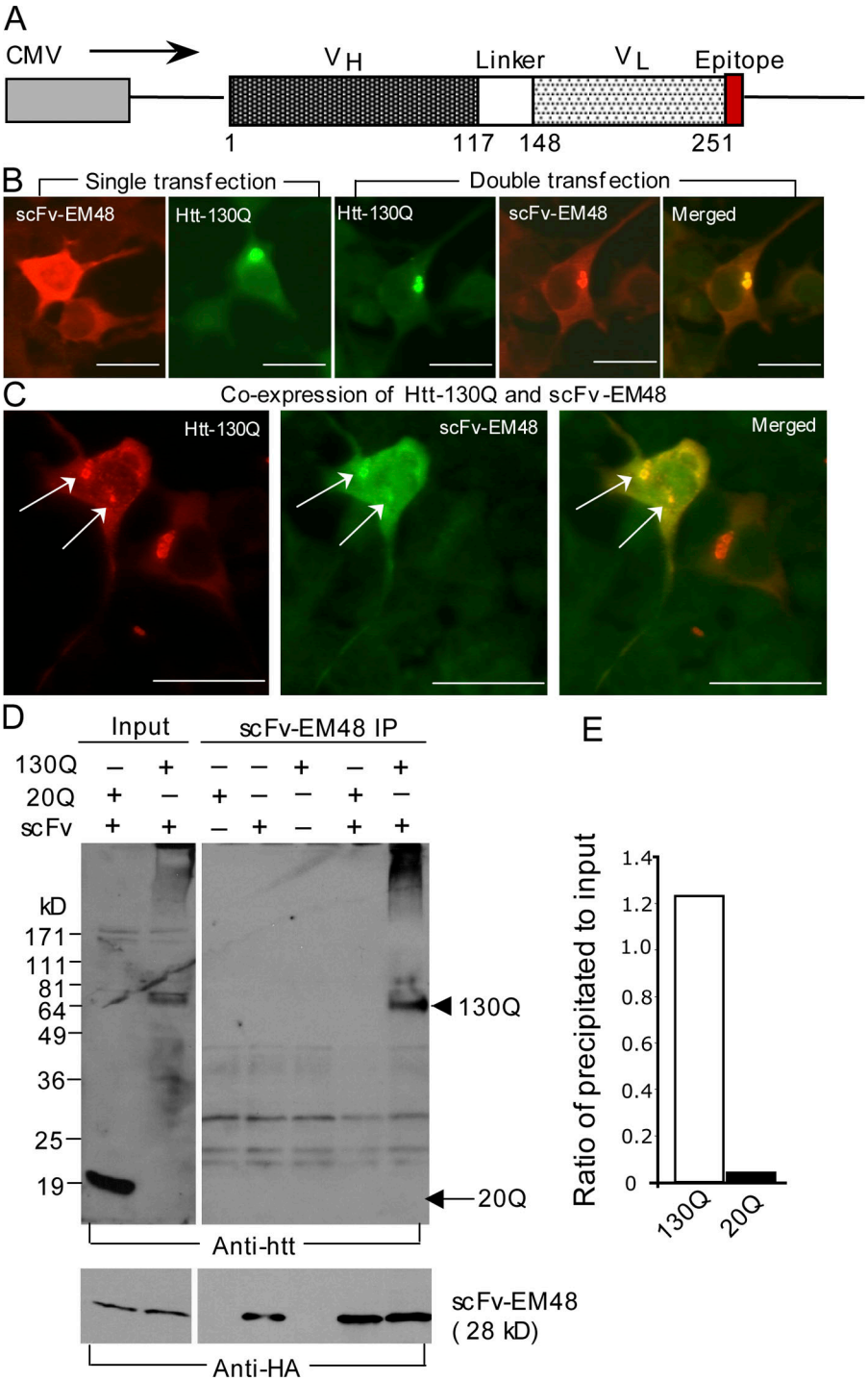

Figure 2. **Generation and expression of scFV-EM48.** (A) Structure of the intrabody scFv-EM48. The intrabody (251 aa) consists of variable region heavy and light (V_H and V_L) chains of the scFv for mEM48, which are linked by a Gly-Ser domain and tagged with the HA epitope. Amino acid numbers are indicated. (B) Expression of scFv-EM48-HA in cultured HEK293 cells. scFv-EM48-HA was either transfected alone or cotransfected with mutant htt (1–208 aa) containing 130Q. Cells were labeled with mouse anti-HA for scFv-EM48 and rabbit EM48 for htt. Note that scFv-EM48 is colocalized with mutant htt (htt-130Q) in cytoplasmic aggregates. (C) Coexpression of scFv-EM48 and mutant htt in cultured rat cortical neurons (arrows) also shows the colocalization of scFv-EM48 with mutant htt. In B and C, cells were immunostained with mouse anti-HA (12CA5) and rabbit EM48. Bars, 10 µm. (D) Western blot analysis of immunoprecipitates from transfected HEK293 cells that express scFv-EM48-HA and exon1 htt with 130Q or 20Q. scFv-EM48 (scFv) was precipitated by the antibody (12CA5) to the HA epitope (bottom). The input and precipitates (IP) were then probed with rabbit EM48 (top). The arrow indicates soluble htt-20Q and the arrowhead indicates htt-130Q. The bracket indicates the stacking gel in which aggregated htt is seen. (E) Densitometry of the ratio of precipitated htt to input from a representative experiment. Similar results were seen in two separate experiments.

more mEM48 immunoreactivity, despite their lesser amounts on the blot (Fig. 1 C).

This increased immunoreaction as a result of polyQ expansion led us to clone the cDNA for mEM48 from its hybridoma cell line, with the aim of expressing this recombinant antibody in cells. We joined cloned cDNAs encoding variable light (V_L) and variable heavy (V_H) chains of mEM48 via an oligonucleotide linker, generating a 750-bp cDNA that encodes a single-chain Fv (scFv) for mEM48. This intrabody (scFv-EM48) was tagged with the HA epitope and expressed under the cytomegalovirus (CMV) promoter (Fig. 2 A). When coexpressed with an N-terminal mutant htt (1–208 aa) containing 130Q, scFv-EM48 colocalized with htt aggregates in both cultured HEK293 cells (Fig. 2 B) and primary cortical neurons (Fig. 2 C). Coexpression of this intrabody with other polyQ disease proteins, such as ataxin-1 and ataxin-7, failed to show any colocalization with polyQ aggregates (Fig. S2, available at http://www.jcb.org/cgi/content/full/jcb.200710158/DC1), which indicates a specific association between scFv-EM48 and htt. We next used coimmunoprecipitation to examine the interaction of scFv-EM48 with htt in transfected cells. Immunoprecipitation of scFv-EM48 pulled down soluble mutant htt

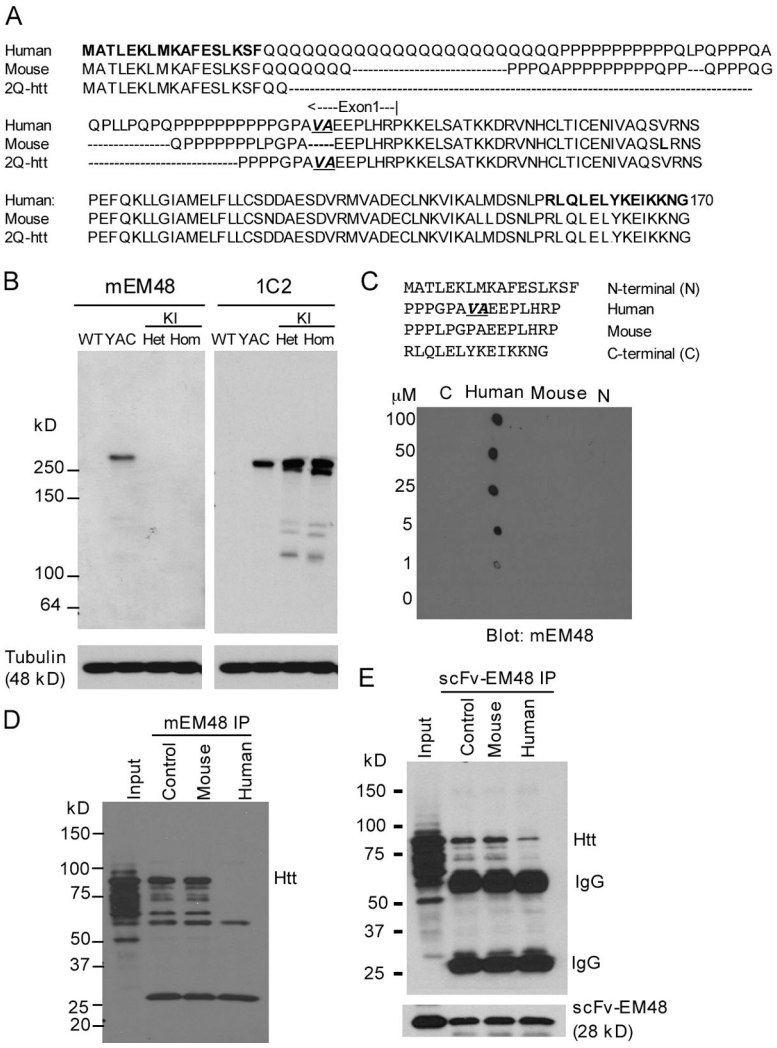

Figure 3. **Identification of the likely epitope for mEM48.** (A) Comparison of N-terminal sequences of human and mouse htt and the antigen 2Q-htt. Two amino acid (VA) residues (italic type and underlined) are located after the polyP tract in human htt and 2Q-htt but are not present in mouse htt. Sequences in bold type were used for synthetic peptides. (B) Western blotting of cerebral cortical tissues from an HD YAC128 mouse, which expresses full-length mutant human htt, and from homozygous (Hom) or heterozygous (Het) HD 150Q knock-in (KI) mice, which express full-length mutant mouse htt. Note that the 1C2 antibody recognizes mouse and human mutant htt, whereas mEM48 only recognizes human mutant htt. (C) Htt sequences shown in A were used to synthesize N-terminal (N), human, mouse, or C-terminal (C) peptides. These peptides were applied to the dot blot at different concentrations (1–100 μM), and the blot was subsequently probed with mEM48. Only the human peptide reacts with mEM48. (D) PC12 cell lysates containing transfected GFP-htt (1–208 aa with 130Q) were immunoprecipitated by mEM48 in the presence of the human or mouse peptide (10 μm). The blot was probed with rabbit EM48. Only the human peptide blocks the immunoprecipitation. Control, immunoprecipitation without peptides. (E) Immunoprecipitation of scFv-EM48-HA in transfected PC12 cells by mouse anti-HA. The blot was probed with mEM48 for the coprecipitated GFP-htt-130Q (top, Htt) and with anti-HA for scFv-EM48 (bottom). The human but not the mouse peptide markedly inhibited the coprecipitation of htt.

in transfected HEK293 cells (Fig. 2 D). Some aggregated htt, which remained in the stacking gel, was coprecipitated with the scFv-EM48 as well, a result that is in agreement with our immunocytochemistry data showing that scFv-EM48 is present in some htt aggregates. More importantly, there was very little normal htt in the immunoprecipitates, despite the fact that a substantial level of transfected normal htt could be detected by rabbit EM48. Densitometry of the ratio of precipitated/input amount also shows that scFv-EM48 binds only weakly to normal htt, whereas it preferentially binds to mutant htt.

The preferential binding of the intrabody to mutant htt proves that the immunoreaction of mEM48 with htt is enhanced by polyQ expansion. Because mEM48 does not react with mouse htt and was generated with an antigen (2Q-htt) that lacks the polyQ and polyP tracts, we reasoned that comparison of the N-terminal sequences of 2Q-htt and htt from human and mouse might provide insight regarding the epitope for mEM48 (Fig. 3 A). Because scFV-EM48 reacts with mutant htt exon1, we focused on the amino acid sequences in exon1 and found that two amino acid residues (VA) located after the polyP tract are present in both human htt and 2Q-htt but not mouse htt. To examine whether mouse mutant htt that carries an expanded polyQ tract also fails to react with mEM48, we performed mEM48 Western blotting of brain tissues from YAC128 mice, which express full-length human mutant htt with 128Q, and HD 150Q knock-in mice, which express full-length mouse mutant htt with 150Q. Although the 1C2 antibody, which reacts with expanded polyQ tracts, recognizes both human and mouse mutant htt, mEM48 only reacts with human mutant htt (Fig. 3 B). To verify that the presence of the VA residues may be critical for mEM48 immunoreaction, we synthesized a short peptide (16 aa) of human htt containing the VA residues (human peptides). For comparison, we used the peptides from the corresponding region of mouse htt that lacks the VA residues (mouse peptides). N-and C-terminal sequences of the first 170 amino acids, which are identical in human and mouse htt, were included as controls. Dot blots demonstrate that only the human peptide binds mEM48 (Fig. 3 C). Moreover, the human but not the mouse peptide can inhibit the coimmunoprecipitation of mutant htt by mEM48 in transfected cells (Fig. 3 D). We also have shown that mutant htt can be precipitated by the intrabody (scFv-EM48) in transfected cells (Fig. 2 D), and this precipitation could be markedly attenuated by the human but not the mouse peptide (Fig. 3 E). As VA residues are present in the human but not the mouse peptides, these findings suggest that the VA residues in exon1 of human htt are likely the epitope for mEM48 and its intrabody. However, the

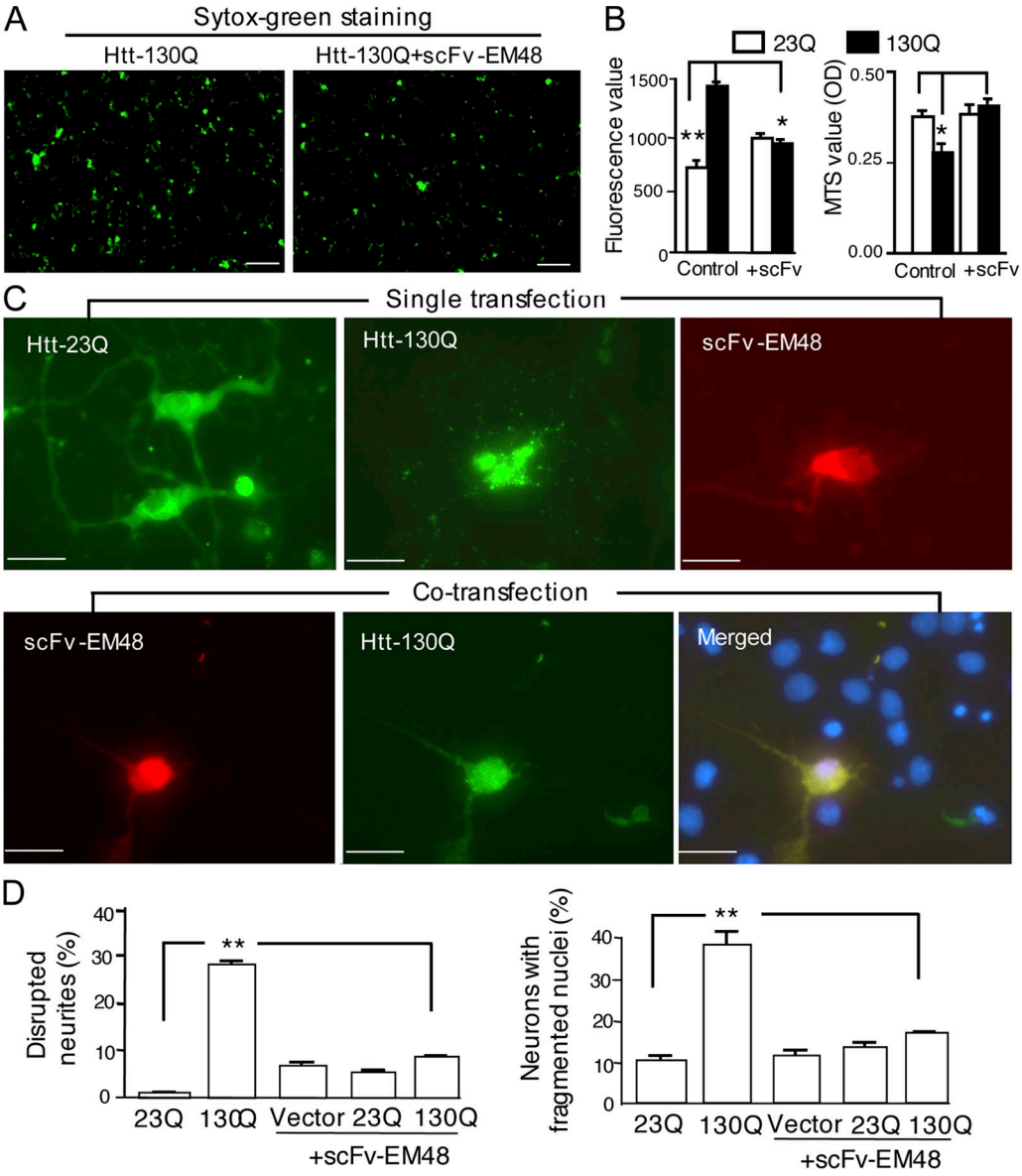

Figure 4. **scFv-EM48 suppresses cytotoxicity of mutant htt.** (A and B) HEK293 cells were transfected with htt (1–208 aa) containing 23Q or 130Q and scFv-EM48 (+scFv). Cotransfection with a vector served as a control. SYTOX green staining of transfected HEK293 cells is shown in A, in which greater fluorescence is correlated with increased cell death. In B, the relative fluorescence values of SYTOX green–containing cells were obtained from six transfection experiments. Cell viability was also measured by a modified MTT assay (MTS) and expressed as absorbance at 490 nm (OD490 nm absorbance values; $n = 9$, $P < 0.05$). The decreased MTS correlates with reduced cell viability. (C) Immunofluorescent staining of cultured rat cortical neurons (7 days in vitro) that express transfected htt (htt-23Q or htt-130Q) or scFv-EM48 alone (top). Htt was labeled by rabbit EM48, and scFv-EM48-HA was labeled by antibody to the HA epitope. Note that mutant htt formed neuritic aggregates and caused neuritic fragmentation in transfected cells. Coexpression of scFv-EM48 reduced htt aggregation in neurites and degeneration of cultured neurons (bottom). Nuclei were stained with Hoechst blue dye in the merged images. (D) The percentage of cells showing disrupted neurites and fragmented nuclei. Data were obtained by counting 156–198 transfected cells in three transfection experiments. The data are presented as means ± standard error. *, $P < 0.05$; **, $P, < 0.01$. Bars: (A) 100 μm; (C) 8 μm.

human sequences that include VA (PPGPAVA) also differ from the mouse sequences (LPGPA) and might also be the source of the preferential immunoreactivity with mEM48.

Intrabody inhibits htt cytotoxicity

If scFv-EM48 indeed binds tightly to mutant human htt, it may prevent htt from binding to other proteins, thereby reducing htt toxicity. We transfected HEK293 cells with N-terminal htt (1–208 aa) that contained either 23Q or 130Q. scFv-EM48 was also coexpressed to assess its protective effect. Approximately 60–70% of HEK293 cells expressed transfected proteins (unpublished data). Using SYTOX green, which labels dying cells, we observed that scFv-EM48 reduced the number of htt-transfected cells stained with SYTOX green compared with cells transfected with mutant htt and vector (Fig. 4, A and B). We also examined the viability of htt-transfected cells using the MTS assay. The expression of htt-130Q reduced cell viability compared with htt-23Q transfection. However, this decrease in viability was improved by coexpression of scFv-EM48 (Fig. 4 B).

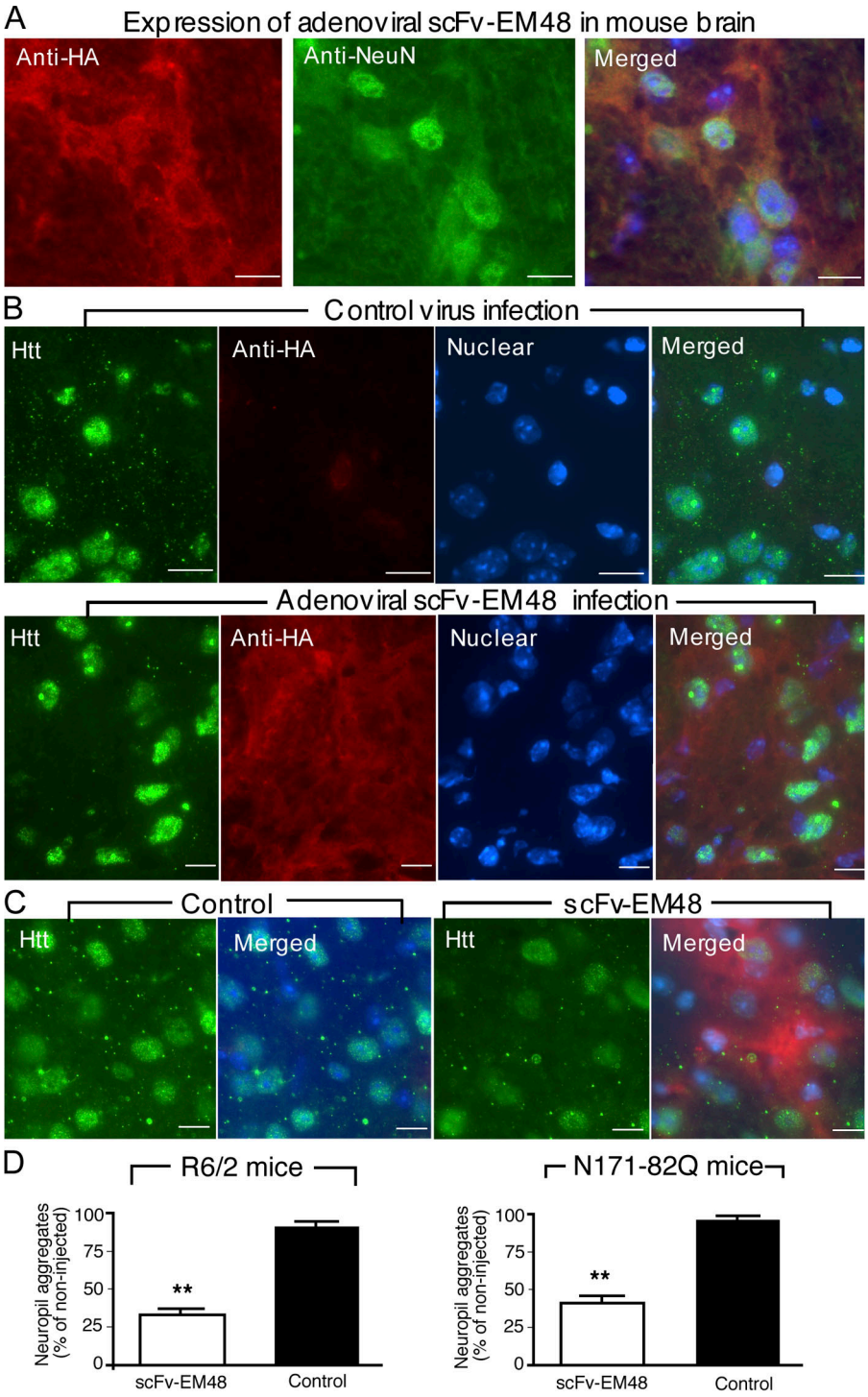

Figure 5. **scFv-EM48 reduces neuropil aggregates in HD mouse brains.** (A) Immunostaining of the mouse brain with rabbit anti-HA (red) and mouse anti-NeuN (green) confirms that scFv-EM48-HA is expressed in neurons. Merged image is also shown. (B and C) Immunostaining of the striatum of R6/2 mice (B) and the cortex of N171-82Q HD mice that were injected with adenoviral vector (control virus) or adenoviral scFv-EM48 (C). Rabbit EM48 was used to stain transgenic htt (green). scFv-EM48 staining is not shown separately but can be seen in the merged images in which scFv-EM48-HA (red) is stained by mouse antibody to the HA epitope, and nuclei (blue) were revealed with Hoechst dye. Note that small neuropil aggregates were decreased in the adenoviral scFv-EM48–injected area. Bars, 5 µm. (D) Quantitative assessment of neuropil aggregate density in R6/2 and N171-82Q mice. The values represent the number of neuropil aggregates per image (630×) relative to the noninjected contralateral area. The data are presented as means ± standard error. **, P <0.01.

To examine whether scFv-EM48 also reduces the neurotoxicity of mutant htt, we cotransfected scFv-EM48 with htt-130Q in cultured rat cortical neurons. Similar to previously published findings (Saudou et al., 1998; Li et al., 2001), mutant htt could lead to neuritic disruption (Fig. 4 C) and pyknotic nuclei (Fig. S3, available at http://www.jcb.org/cgi/content/full/jcb.200710158/DC1). Expression of scFv-EM48 alone did not affect the morphology of cultured neurons, but its coexpression with htt-130Q significantly reduced the number of htt-transfected neurons with disrupted neurites or fragmented nuclei (Fig. 4, C and D; and S3).

Intrabody suppresses neuropil aggregates in HD mouse brain

Although the results in Fig. 4 established the protective effects of scFv-EM48 in cultured cells, whether scFv-EM48 could confer protection in HD mouse brains remained to be seen. To test the effects of scFv-EM48 in the brain, the protein must be delivered via viral infection and microinjection of a small volume (1–2 µl per injection). However, conventional adenoviral and lentiviral vectors failed to yield a sufficiently high titer of viral scFv-EM48. Intrabody instability

in cells and viral toxicity very likely impose a considerable obstacle to using these viral vectors. Next, we tried a helper-dependent adenoviral vector in which the viral coding sequences have been replaced with noncoding human genomic DNA (Toietta et al., 2002, 2005). The elimination of all viral protein-coding sequences in this vector results in less cytotoxicity and long-term expression of transgenes compared with the earlier-generation adenoviral vectors (Toietta et al., 2002, 2005). Western blot analysis confirmed that this adenoviral vector expressed scFv-EM48 protein of the correct size in cultured cells (Fig. S4, available at http://www.jcb.org/cgi/content/full/jcb.200710158/DC1).

Using immunofluorescence double-labeling with antibodies to the HA epitope and to a neuronal marker (NeuN), we first confirmed that scFv-EM48 was expressed in neurons after microinjection into the mouse brain (Fig. 5 A). Unlike transfected cells, in which mutant htt can form large inclusions in the cell bodies, neurons in HD brains show aggregates in the nucleus and neuronal processes (DiFiglia et al., 1997; Gutekunst et al., 1999; Li et al., 1999). After confirmation of neuronal scFv-EM48 expression, we next injected adenoviral scFv-EM48 into the striatum of 7-wk-old R6/2 mice. At this age, R6/2 mice begin to develop prominent htt nuclear and neuropil aggregates, and stereotaxic injection into the mouse striatum becomes feasible. 4 wk after the procedure, we found that the number of neuropil aggregates in the injected area had been reduced dramatically when compared with the noninjected region (Fig. 5 B). There appeared to be a slight reduction of nuclear staining as well, but this difference was difficult to quantify by immunostaining.

We also injected adenoviral scFv-EM48 into N171-82Q mice. This HD mouse model expresses the first 171 amino acids of human htt with 82Q and also demonstrates obvious neuropil aggregates in the brain (Schilling et al., 1999). We found that adenoviral scFv-EM48 injected into the cortex of N171-82Q mice over a period of 6 wk reduced the abundance of neuropil aggregates (Fig. 5 C).

To verify the specificity of adenoviral scFv-EM48, we also injected mice from both strains with a control virus that does not express scFv-EM48. We quantified the neuropil aggregate density per image (630×) and normalized this quantity by the density of neuropil aggregates in the noninjected contralateral region. This method allowed us to mitigate the influence of variations in immunostaining and brain section preparation. Compared with control virus, injection of adenoviral scFv-EM48 significantly reduced neuropil aggregates in R6/2 and N171-82Q mouse brains ($P < 0.01$; $n = 10$ for adenoviral scFv-EM48 vs. $n = 6$ for control; Fig. 5 D).

Both R6/2 and N171-82Q mice widely express mutant htt in various brain regions. As a result, they develop severe neurological symptoms and early death by the age of 3–6 mo (Davies et al., 1997; Schilling et al., 1999). However, inhibiting the expression of transgenic htt via siRNA in the striatum of N171-82Q mice, which exhibit a slower disease progression than R6/2 mice, leads to an improvement in their motor function (Harper et al., 2005). Therefore, we speculated that N171-82Q mice would also be good candidates for testing the in vivo protective effects of scFv-EM48 after its delivery to the striatum. To this end, we bilaterally injected adenoviral scFv-EM48 into the striatum (1.25 µl per site) of 10-wk-old N171-82Q mice. As a control, HD mice were injected with the same amount of adenoviral vector. After 8 wk, we observed significant improvements in gait function for the HD mice that had been injected with adenoviral scFv-EM48 (Fig. 6, A and B). Measures included stride length (50.82 ± 1.95 mm [$n = 11$] for scFv-EM48 vs. 42.8 ± 3.1 mm [$n = 9$] for control virus; $P < 0.05$). Also, the RotaRod performance of HD mice was improved. For example, the times on the RotaRod were 93.7 ± 4.32 s ($n = 10$) for scFv-EM48–injected mice and 59.8 ± 1.39 s ($n = 9$) for control virus-injected mice ($P < 0.05$) on trial day 3 (Fig. 6 C). However, we did not observe a significant improvement in body weight or survival of N171-82Q mice injected with adenoviral scFv-EM48 (Fig. 6 D). The selective protection of scFv-EM48 against motor deficits is likely caused by the limited expression of this intrabody in the striatum and its selective effect on cytoplasmic mutant htt. This finding also suggests that the expression of mutant htt in the nucleus and in brain regions other than the striatum can contribute to severe neurological phenotypes.

We also performed immunofluorescence double-labeling of viral-infected PC12 cells and found that scFv-EM48 decreased the number of htt aggregates in neurites (Fig. 7, A and B). To verify that scFv-EM48 reduces the distribution of soluble mutant htt in the neurites, we measured the ratio of htt's neuritic signal to its cell body signal (McGuire et al., 2006). As expected, scFv-EM48 significantly decreased the number of cells with neuritic aggregates (38.8 ± 3.7% for vector control vs. 9.2 ± 0.5% for scFv-EM48; $n = 3$; $P < 0.01$). Also, the relative neuritic distribution of mutant htt in PC12 cells was reduced by scFv-EM48 (ratio of neuritic signal/cell body signal: 0.35 ± 0.06 for scFv-EM48 vs. 0.82 ± 0.04 for vector control; $n = 10$; $P < 0.01$; Fig. 7 C). These findings are consistent with the in vivo inhibition of neuropil aggregates by scFv-EM48 in HD mouse brains (Fig. 5) and in cultured cortical neurons (Fig. S3).

Intrabody promotes the degradation of mutant htt

The significant reduction of neuropil aggregates and the improvement in neurological symptoms associated with scFv-EM48 led us to explore the mechanism underlying this protection. The decreased amount of neuropil aggregates in HD mouse brains could be caused by the reduced distribution of mutant htt to neuronal processes and/or increased htt clearance in the cytoplasm. We therefore fractionated synaptosomes from the striatal tissue of N171-82Q mice, in which the protein level of mutant htt is comparable to endogenous htt (Schilling et al., 1999). As shown previously (Schilling et al., 1999), a cleavage product smaller than transgenic mutant htt (~47 kD) is visible in the brain lysates of HD mice. In HD striatal tissues expressing scFv-EM48, this cleaved product and two additional smaller products (Fig. 8 A, arrowheads) are more abundant than in those brains injected with control adenovirus. This difference suggests that the interaction of the intrabody with mutant htt in the cytosolic region may facilitate the degradation

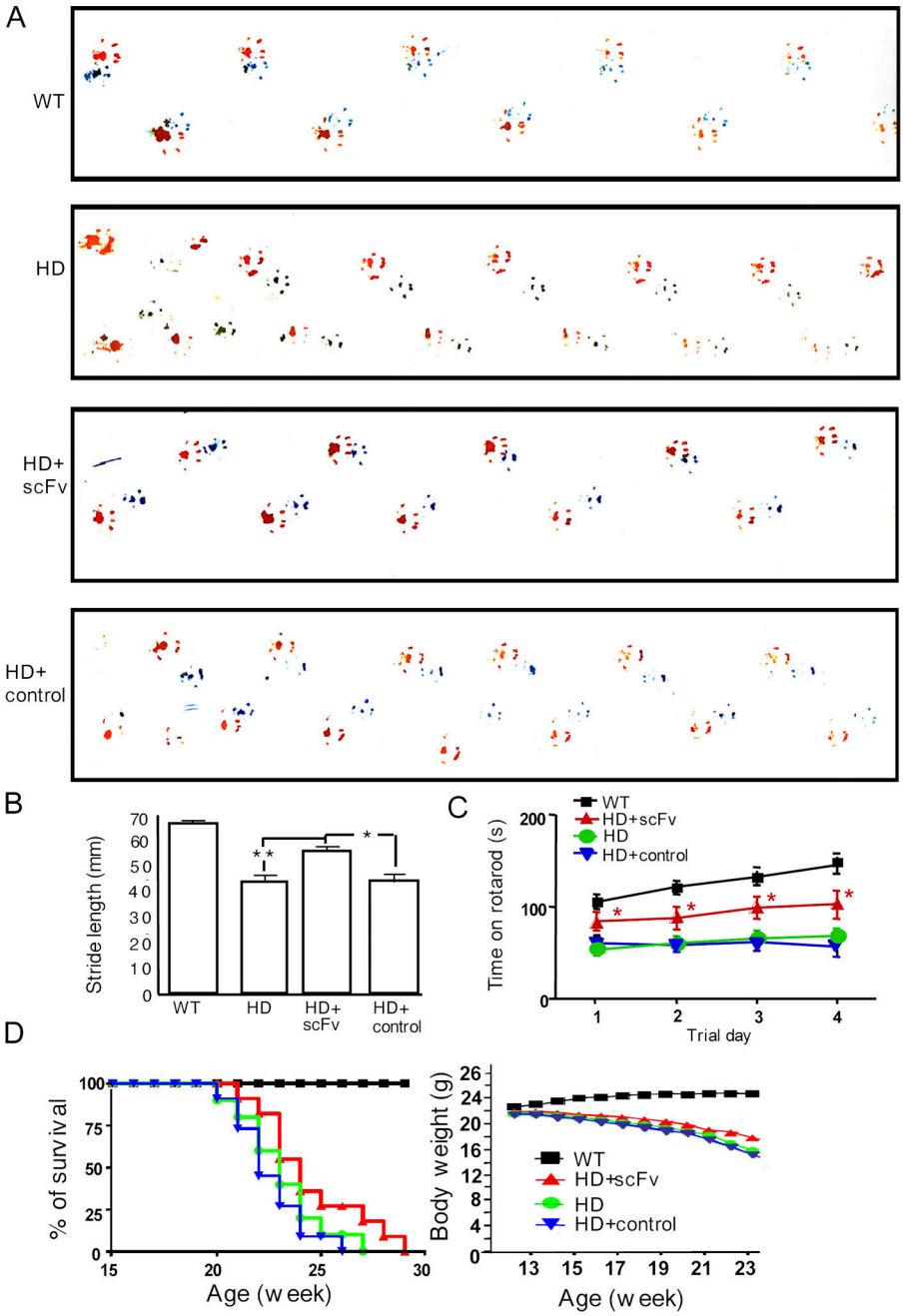

Figure 6. **scFv-EM48 alleviates the motor deficits of N171-82Q mice.** (A) Footprint tracings of wild-type (WT), N171-82Q mice (HD), and N171-82Q mice injected with adenoviral scFv-EM48 (HD + scFv) or an adenoviral vector (HD + control). (B) Mean stride lengths (in millimeters) of the mice in A show that the abnormal gait seen in N171-82Q mice is partially reversed by adenoviral scFv-EM48. (C) Accelerating RotaRod testing of wild-type (WT) and N171-82Q mice (HD) demonstrates an improvement in RotaRod performance (time on the rod) for N171-82Q mice (HD + scFv) that had received adenoviral scFv-EM48 injections in their striatum. In all trials, n = 9–11 mice. $P < 0.05$ as compared with N171-82Q mice injected with adenoviral vector control (HD + control). (D) Survival plot and body weight (in grams) of wild-type (WT), N171-82Q (HD), and N171-82Q mice injected with adenoviral scFv-EM48 (HD + scFv) or an adenoviral vector (HD + control). The data are presented as means ± standard error. *, $P < 0.05$; **, $P < 0.01$.

of mutant htt. Importantly, compared with the samples from HD mice that were injected with adenoviral vector, the ratio (mean ± SEM, $n = 3$) of either soluble (control vs. scFv-EM48: 0.528 ± 0.04 vs. 0.279 ± 0.03, respectively) or oligomeric (1.28 ± 0.11 vs. 0.77 ± 0.06) htt to the synaptic protein syntaxin is decreased in the synaptosomal fractions of HD mice that had been injected with adenoviral scFv-EM48 (Fig. 8 A, bottom). Because the intrabody cannot enter the nucleus to affect nuclear mutant htt, there was no significant difference in the levels of aggregated htt in nuclear fractions of HD mice injected with adenoviral control vector or scFv-EM48 (Fig. 8 A). Thus, this in vivo evidence also indicates that scFv-EM48 can reduce the distribution of mutant htt in nerve terminals in HD mouse brains.

The increased htt degradation in synaptosomes of HD mice injected with adenoviral scFv-EM48 led us to test the possibility that scFv-EM48 can promote the degradation of mutant htt. We coexpressed adenoviral vector or scFv-EM48 with GFP-htt-130Q (1–208 aa with 130Q) in cultured PC12 cells. GFP-htt-130Q is mainly distributed in the cytoplasm and forms cytoplasmic aggregates. Thus, cytoplasmic proteins of PC12 cells were isolated as soluble and nonsoluble or pellet fractions, with the expectation that the latter would be enriched for aggregated htt or htt that is bound tightly to the intrabody. Total cell lysates containing scFv-EM48 show more degraded htt products than control cell lysates (Fig. 8 B). Consistent with the fact that more scFv-EM48 was present in the pellet fraction than in the soluble fraction, more degraded htt products were also

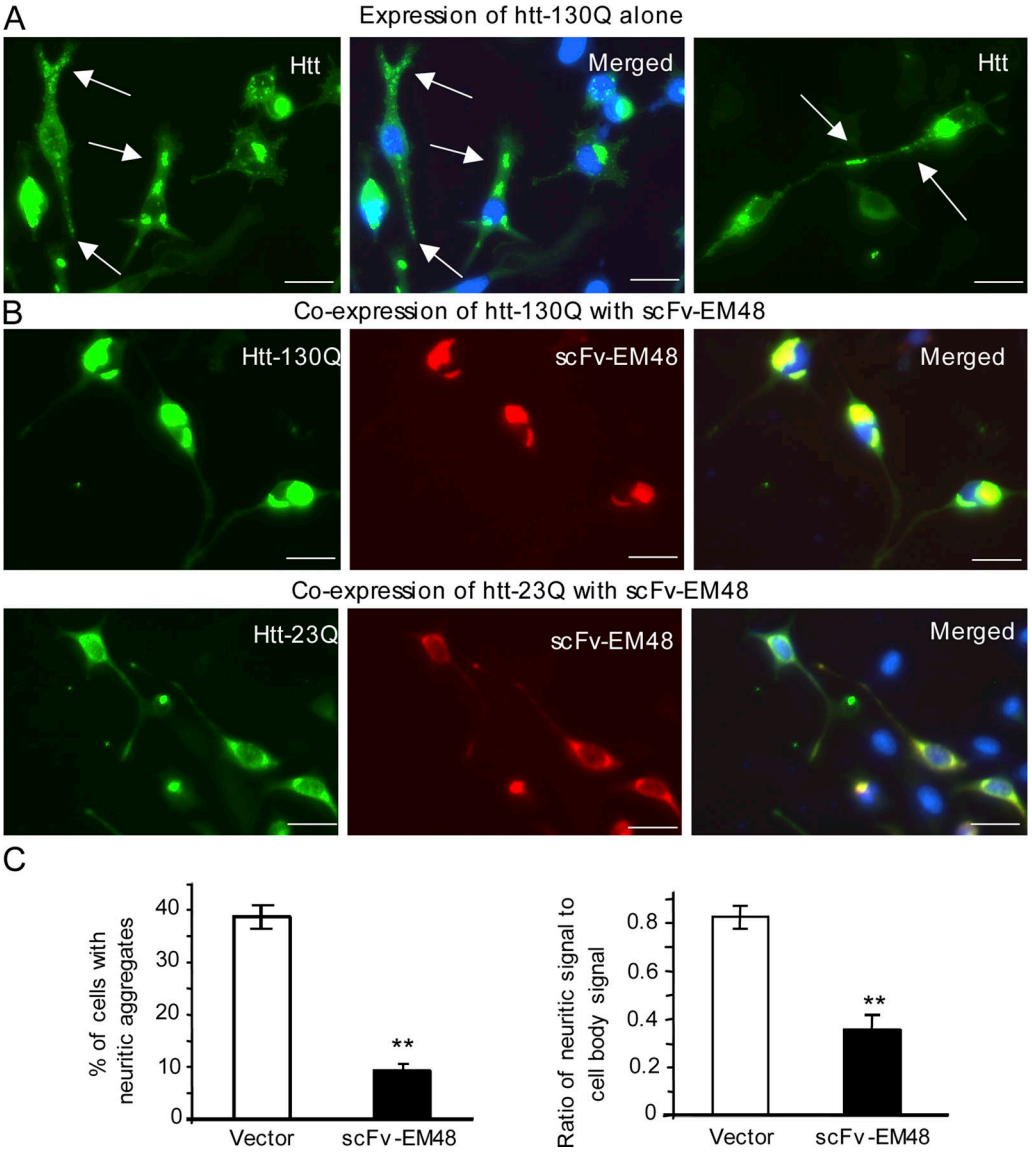

Figure 7. **scFv-EM48 reduces the distribution of mutant htt in the neurites of PC12 cells.** (A) PC12 cells were infected by adenoviral htt-130Q only. Two images (right and left) from independent experiments are shown. The middle image is a merged image showing nuclear (blue) staining for the left image. Arrows indicate htt aggregates in neurites. (B) PC12 cells were coinfected with adenoviral htt and adenoviral scFv-EM48-HA and then stained with rabbit EM48 for htt and mouse anti-HA for scFv-EM48. (top) Cells coexpressing htt-130Q and scFv-EM48. (bottom) Cells coexpressing htt-23Q and scFv-EM48. Note that the neuritic aggregates formed by htt-130Q are reduced by scFv-EM48. Bars, 10 μm. (C) Quantitative assessment of the percentage of transfected PC12 cells showing neuritic aggregates and the ratios of neuritic htt signals to cell body signals. The data are presented as means ± standard error. **, $P < 0.01$.

detected in the pellet fraction, which suggests that the association of scFv-EM48 with mutant htt is required for the degradation of mutant htt. We then performed pulse-chase experiments to measure the half-life of mutant htt. In the presence of scFv-EM48, the half-life of mutant htt is obviously shorter than in the absence of scFv-EM48 (Fig. 8 C). For example, at 4 h after chasing, 46.9 ± 2.62% of radiolabeled mutant htt remained in the presence of scFv-EM48 compared with 74.1 ± 3.2% ($P < 0.05$, $n = 3$) of mutant htt in the absence of scFv-EM48 ($P < 0.05$, $n = 3$). It is possible that the binding of scFv-EM48 alters the conformation of mutant htt and leads to its degradation via the ubiquitin–proteasome system. If true, we should see increased ubiquitination of mutant htt in the presence of scFv-EM48. Because the cytoplasmic nonsoluble or pellet fraction is enriched in mutant htt and scFV-EM48 without detectable tubulin (Fig. 8 B), we probed this fraction with an antibody to ubiquitin and observed an obvious increase in the amount of ubiquitinated products (Fig. 8 D, left). Immunoprecipitation of htt by EM48 also shows more ubiquitinated products in the presence of scFv-EM48 (Fig. 8 D, right). These findings are consistent with the increased degradation of mutant htt in the pellet fraction seen in Fig. 8 B. To provide direct evidence that scFv-EM48 increases the ubiquitination of mutant htt, we performed immunofluorescent staining of PC12 cells that were infected by adenoviral GFP-htt-130Q alone or with adenoviral scFv-EM48. More infected cells contained ubiquitinated aggregates in the presence of scFv-EM48 (73.9 ± 2.4%) than in the absence of scFv-EM48 (49.8 ± 2.8%; $P < 0.05$, $n = 3$; Fig. 8 E).

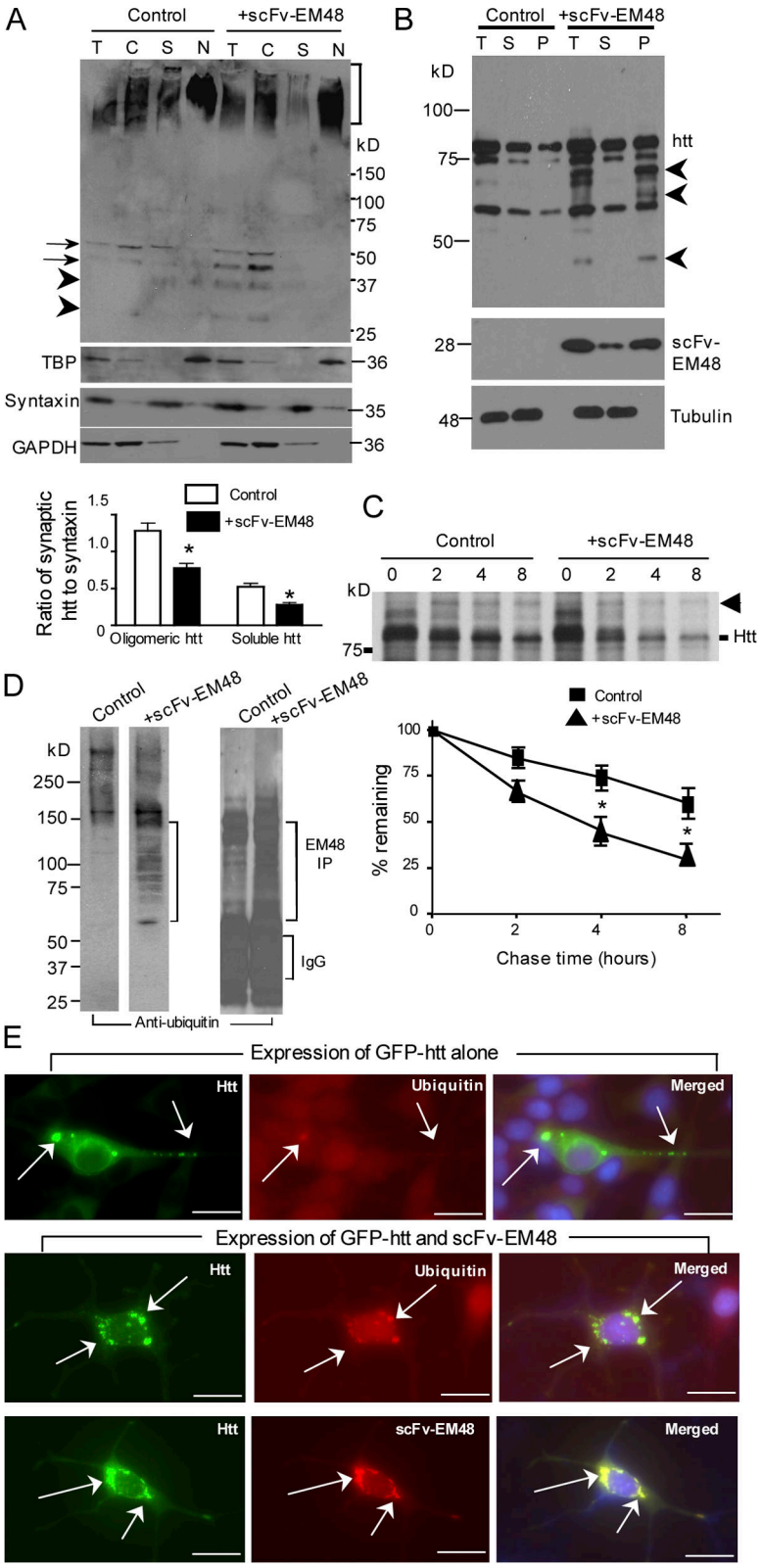

Figure 8. **ScFV-EM48 promotes the degradation of mutant htt.** (A) Western blot of total lysates (T) and cytosolic (C), synaptosomal (S), and nuclear (N) fractions of striatal tissues from N171-82Q mice that had been injected with adenoviral vector (control) or scFv-EM48. Oligomeric mutant htt is present in the stacking gel (bracket). Arrows indicate transgenic htt and its cleaved product and arrowheads indicate additional degraded products. The same samples were probed with rabbit EM48 to htt and antibodies to the synaptic protein syntaxin, the nuclear protein TBP, and the cytoplasmic protein glyceraldehyde-3-phosphate dehydrogenase (GAPDH). The ratios (mean ± SEM, $n = 3$) of oligomeric or soluble htt to syntaxin were obtained using densitometry and are presented beneath the blots. *, $P < 0.05$. (B) Total lysates (T), cytoplasmic soluble (S), and pellet (P) fractions of PC12 cells coinfected by adenoviral GFP-htt-130Q and adenoviral vector (control) or scFv-EM48 were analyzed by Western blotting with mEM48 and antibodies to HA for scFV-EM48 or tubulin. Arrowheads indicate degraded htt products. (C) Pulse chase of mutant htt (GFP-htt-130Q) in adenoviral vector (control)– or scFv-EM48–infected PC12 cells (top). Arrowhead indicates a nonspecific band. Quantification of the percentage of remaining ^{35}S-labeled htt signal at different chase times (bottom, $n = 3$). *, $P < 0.05$. (D) The pellet fractions described in B were analyzed by Western blotting with anti-ubiquitin (left) or subjected to EM48 immunoprecipitation (right). The precipitates were analyzed by Western blotting with anti-ubiquitin. The brackets indicate the increased amount of ubiquitinated products in the presence of scFv-EM48. Precipitated IgG is also indicated. (E) Immunofluorescent staining of PC12 cells, which express GFP-htt-130Q alone or with scFV-EM48, with rabbit anti-ubiquitin and mEM48 or mouse anti-HA. In the absence of scFv-EM48, mutant htt forms aggregates (arrows) that localize to the cell body and neurites (top). In the presence of scFV-EM48, htt aggregates (arrows) remain in the cell body and can be labeled by antibodies to ubiquitin (middle) or to the HA epitope in scFv-EM48 (bottom). Bars, 8 µm.

In control cells that only expressed mutant htt, htt aggregates, which were either ubiquitin negative or weakly labeled by anti-ubiquitin, were also found in neurites, in contrast to scFV-EM48–containing cells in which most htt aggregates were ubiquitinated and remained in the cell body. Using a control intrabody (NAC32) against α-synuclein (Lynch et al., 2008), we found that this control intrabody neither associated with htt aggregates nor reduced htt levels in transfected cells (Fig. S5, available at http://www.jcb.org/cgi/content/full/jcb.200710158/DC1). Collectively, these results indicate that the intrabody scFv-EM48

can reduce the accumulation of mutant htt in neuronal processes while promoting the ubiquitination and degradation of mutant htt in the cytoplasm.

Discussion

Here, we demonstrate that the intrabody scFv-EM48 preferentially binds mutant htt and inhibits the specific neuropathology of HD. This intrabody provides a useful tool for suppressing the cytoplasmic toxicity of mutant htt, thereby allowing us to differentiate the cytoplasmic from the nuclear effects of mutant htt. The present study also suggests that the abnormal conformation of mutant htt itself makes an effective therapeutic target that is highly specific.

Normal levels of htt are critical for neurogenesis and embryonic development (White et al., 1997), and conditional knockout mice, in which htt expression has been inactivated, show degeneration of neuronal cells (Dragatsis et al., 2000). Although these findings suggest that a loss of function may be involved in HD pathology, there is considerable evidence that the polyQ expansion in mutant htt results in a gain of toxic function. For example, even in those HD mouse models expressing endogenous htt at normal levels, transgenic mutant htt leads to neuropathology and neurological symptoms (Davies et al., 1997; Schilling et al., 1999; Graham et al., 2006). The gain-of-toxic-function theory provides a rationale for suppressing the expression of the transgene in HD mice (Yamamoto et al., 2000; Harper et al., 2005). However, such suppression cannot distinguish the effects of mutant htt in the nucleus versus the cytoplasm. An alternative approach has been targeting nuclear export sequences to transgenic polyQ proteins, but expanded polyQ proteins could not be completely directed to the cytoplasm (Jackson et al., 2003; Benn et al., 2005).

Intracellular expression of intrabodies has proved successful at blocking the toxic effects of mutated proteins or pathogenic agents with high selectivity (Hudson and Souriau, 2003; Lobato and Rabbitts, 2004). The interaction of intrabodies with their targets can prevent the binding of these targets to other proteins (Dorai et al., 1994). Furthermore, intrabodies in both cellular and *Drosophila melanogaster* HD models have shown encouraging protective effects (Lecerf et al., 2001; Khoshnan et al., 2002; Colby et al., 2004; Miller et al., 2005; Wolfgang et al., 2005), but such studies have not been extended to HD mouse brains. Unlike most intrabodies used previously, our intrabody scFv-EM48 binds to a unique epitope in human htt and preferentially interacts with mutant htt. Because the polyQ domain is not the epitope for this interaction, the expanded polyQ-mediated conformational alteration must lead to the increased binding of mutant htt to scFv-EM48. This is also consistent with the notion that polyQ expansion enhances the interactions of mutant htt with other molecules. This unique property allows for the selective reduction of mutant htt and its toxic effects, without interfering with the critical function of normal htt. In support of this idea, we provide in vivo evidence that scFv-EM48 can suppress formation of neuropil aggregates in the brain and ameliorate neurological symptoms in N171-82Q mice, in which transgenic mutant htt forms abundant neuropil aggregates (Schilling et al., 1999). In addition, the in vivo effect of scFv-EM48 on mutant htt is persuasively indicated by its preferential binding to mutant htt and its in vitro protection against htt toxicity.

We found that scFv-EM48 did not significantly reduce the formation of nuclear inclusions. It is conceivable that cytoplasmic scFv-EM48 cannot enter the nucleus, where these htt fragments have already accumulated. Alternatively, small htt fragments can readily enter the nucleus, and expanded polyQ tracts prevent their export from the nucleus (Cornett et al., 2005), whereas the transport of mutant htt to neuronal processes is dependent on its interactions with trafficking proteins. Although scFv-EM48 binds an epitope that may not be involved in interactions with other proteins, its interaction with mutant htt can cause a conformational change that could alter the association of htt with other proteins, such as trafficking proteins. Importantly, interactions of intrabody with htt can alter the stability of htt, as our studies demonstrate that the interaction of scFv-EM48 with mutant htt increases the ubiquitination of mutant htt and reduces its half-life. It has been shown previously that some intrabodies can reduce htt aggregation (Lecerf et al., 2001; Khoshnan et al., 2002; Colby et al., 2004) or decrease the level of exon1 mutant htt (Wolfgang et al., 2005). Our findings suggest that the interaction of scFv-EM48 with mutant htt could alter htt's conformation and/or make mutant htt more accessible to the ubiquitin–proteasome system, thereby promoting its degradation. It would be interesting to investigate whether previously reported htt intrabodies also act on htt via this mechanism.

It is known that cytoplasmic mutant htt is transported within neuronal processes (Gunawardena et al., 2003; Szebenyi et al., 2003). In the present study, we present the first in vivo evidence that the interaction of intrabody with cytoplasmic mutant htt reduces its distribution in the neuronal processes and ameliorates neurological symptoms in HD mice. Decreasing the distribution of mutant htt in neuronal processes can reduce the cytoplasmic effects of htt on mitochondria, trafficking, and synaptic transmission to improve neuronal function. Suppressing neuropil aggregate formation may be particularly relevant in treating the specific neuropathology of both HD and spinobulbar muscular atrophy, in which neuropil aggregates have also been observed (Parker et al., 2001; Piccioni et al., 2002). Although soluble mutant htt can affect intracellular trafficking (Gunawardena et al., 2003; Szebenyi et al., 2003; Gauthier et al., 2004; Trushina et al., 2004), polyQ aggregates in the neuronal processes can also physically block intracellular transport (Piccioni et al., 2002; Lee et al., 2004; Chang et al., 2006) and are associated with axonal degeneration in polyQ disease models (Li et al., 2001; Parker et al., 2001; Yu et al., 2003). Because neuropil aggregates are more abundant than nuclear inclusions in the brains of presymptomatic and early-stage HD patients (Gutekunst et al., 1999), suppressing their formation could be beneficial in terms of reducing neuronal dysfunction before degeneration occurs. Because we have shown that scFv-EM48 is specific to mutant htt, the present findings suggest that intracellular antibodies to specific polyQ proteins can make useful tools for unraveling pathological events caused by polyQ proteins, and may also pave the way for development of effective polyQ disease therapies.

Materials and methods

Reagents and animals

Transgenic mice (R6/2 and N171-82Q) were obtained from The Jackson Laboratory and maintained in the animal facility at Emory University. Cerebral cortical tissues from YAC128 transgenic mice were provided by M. Hayden (University of British Columbia, Vancouver, Canada). Brain tissues from HD 150Q knock-in mice were obtained as described previously (Zhou et al., 2003). Htt peptides (14–18 residues) from different regions of N-terminal human and mouse htt were synthesized by the Biochemical Core Facility at Emory University. In vitro synthesized htt was generated in 50 µl of in vitro SP6-Transcription/Translation kit (Roche) with [^{35}S]methionine and PRK plasmids (1 µg each) encoding different forms of htt. The reaction was incubated at 30°C for 1 h. 20 µl of reaction was subjected to SDS-PAGE. The rabbit and mouse antibodies to htt were generated as described previously (Zhou et al., 2003). Other antibodies used include mouse monoclonal antibodies to γ-tubulin (Sigma-Aldrich), NeuN (Millipore), syntaxin (Sigma-Aldrich), TBP (Santa Cruz Biotechnology, Inc.), GAPDH (Millipore), and ubiquitin (Dako). PRK expression vectors encoding N-terminal htt (208 aa) with 23Q or 130Q and adenoviral htt constructs encoding GFP–N-terminal htt (1–208 aa) with 23Q or 130Q were described previously (Shin et al., 2005). FLAG-tagged pcDNA–ataxin-1 82Q plasmid was provided by H.T. Orr (University of Minnesota, Minneapolis, MN). Myc-tagged CMV–ataxin-7 92Q plasmid was provided by A. La Spada (University of Washington, Seattle, WA).

Generation and expression of scFv-EM48

RNAs from hybridoma cells were used for RT-PCR with primers complementary to the consensus sequences flanking the variable region heavy and light (V_H and V_L) chains of mouse IgG (GE Healthcare). Cloned scFv cDNAs encoding V_L (320 bp) and V_H (340 bp) chains of mEM48 were linked by a 45-bp oligonucleotide encoding Gly-Ser (Khoshnan et al., 2002), generating a 750-bp cDNA that encodes scFv-EM48. The cDNA was linked with the influenza HA or FLAG epitope and inserted into the PRK vector containing the CMV promoter for expression in cultured cells. A plasmid encoding the control intrabody (NAC32-myc) was provided by A. Messer (Wadsworth Center, New York State Department of Health, Albany, NY). HEK293 cells and cultured primary neurons from the cerebral cortex of embryonic day 17 or 18 rat fetuses were transfected with scFv-EM48 using Lipofectamine 2000 (Invitrogen).

For expression of scFv-EM48 via adenoviral vector, we used a helper-dependent adenoviral vector that contained the CMV promoter, scFv-EM48 cDNA, the woodchuck hepatitis virus posttranscriptional regulatory element, and the bovine-globin polyadenylation site. The expression cassette was cloned into pBGShuttle, and the corresponding adenovirus backbone was generated by homologous recombination in *Escherichia coli*, as described previously (Shin et al., 2005). Generation and purification of virus were performed as described previously (Toietta et al., 2002, 2005). We were able to generate viral scFv-EM48 with a titer of 10^{12} viral particles per milliliter. Adenoviral vector that did not express scFV-EM48 served as a control.

Cell viability studies

HEK293 cells were grown in 6-well plates to 60–70% confluence. After 48 h transfection, cells were collected and then resuspended in serum-free medium. We dispensed 50 µl of the cell suspension (5,000 cells) into a 96-well plate. Cell viability was determined by a modified 3-(4,5-dimethylthiazol-2-yl)-2,5-diphenyltetrazolium bromide (MTT) assay, the MTS assay (CellTiter 96; Promega), as described previously (Zhou et al., 2003). For the SYTOX green staining assay, 0.3 µl of the 5 mM SYTOX green stain solution (Invitrogen) was added to each well of transfected cells after 48 h transfection in a 6-well plate. Cells were incubated at 37°C in an atmosphere of 5% CO_2 for 15 min and washed three times with serum-free media. Cells (10^6 per 100 µl) were transferred to a 96-well plate for measuring fluorescence using a fluorescent reader (FLUOstar Galaxy; BMG Labtech GmbH) with an excitation wavelength of 485 nm and an emission wavelength of 520 nm. For studying primary cultured cortical neurons, these cells (5 d in vitro) were transfected with PRK-scFv-EM48 and a PRK vector containing N-terminal htt (208 aa) with 130Q or 23Q on day 5 of culture. After 48 h transfection, the transfected cells were fixed with 4% paraformaldehyde and examined using fluorescence immunocytochemistry. Cells were stained with rabbit antibody (EM48) to htt, mouse antibody to the HA epitope in scFv-EM48, and Hoechst dye for detection of nuclei. We counted the number of neurons with disrupted neurites or fragmented nuclei under a fluorescence microscope (Axiovert 200 MOT; Carl Zeiss, Inc.) and a 63× LD-Achroplan 0.75 lens (Carl Zeiss, Inc.). The images were captured with a digital camera (Orca-100; Hamamatsu) and Openlab software (PerkinElmer). We performed quantification of htt aggregates and htt signal in neurites and the cell body of PC12 cells using the same method described previously (McGuire et al., 2006). We counted 10 different fields from each sample. Data were obtained by counting 81–93 cells per group in three experiments and are presented as the percentage of cells with disrupted neurites or fragmented nuclei.

Stereotaxic injection of scFv-EM48 into mouse brain

We anesthetized mice with intraperitoneal injections of 2.5% avertin (0.012 ml/g body weight) and performed lateral stereotaxic injections of viral vectors. Using a 5-µl syringe (Hamilton), we injected 1.25 µl of adenoviral scFv-EM48 or control viral vector (6×10^9 viral particles per microliter) into the striatum or cortex according to the following coordinates: for the striatum, 0.8 mm rostral to bregma, 2.0 mm lateral to the midline, and 3.5 mm ventral to the dural surface; for the cortex, 1 mm rostral to bregma, 2.0 mm lateral to the midline, and 1.5 mm ventral to the dural surface. The injection rate was 0.5 µl/2 min, and the needle was left in place for an additional 5 min before being removed. Body weight, growth, behavior, and motor function were examined using standard assays (Davies et al., 1997; Schilling et al., 1999). After 4–6 wk, the injected animals were killed and subjected to immunohistochemical staining. The density of neuropil aggregates was determined by counting the number of htt-positive aggregates per image, and this is represented as a percentage of the noninjected contralateral region. The adenoviral scFv-EM48–injected group contained 10 mice, whereas the control adenoviral vector–injected group consisted of six mice.

Microscopy

All imaging was done at room temperature, ∼26°C. Immunocytochemical analysis of cultured cells and mouse brain tissues was performed as described previously (Li et al., 2000, Shin et al., 2005). Light micrographs were taken using a microscope (Axiovert 200 MOT) equipped with a digital camera (Orca-100) and image acquisition software (Openlab). A 20× LD-Achroplan 0.4 NA or 63× 0.75 NA oil immersion objective lens (both from Carl Zeiss, Inc.) was used for light microscopy. For immunofluorescent staining, species-specific fluorescein- or Texas red–conjugated secondary antibodies (Jackson ImmunoResearch Laboratories) were applied for 1 h at room temperature followed by counterstaining with Hoechst dye. Enhanced GFP was imaged using 488-nm excitation and a 500–530-nm band-pass filter, and RFP was imaged using 543-nm excitation and a 565–615-nm band-pass filter. The figures were created using Photoshop 7.0 software (Adobe) and, in some cases where the brightness and contrast of the whole image needed adjustment, we used the brightness/contrast adjustment function.

Behavioral analysis

To examine gait function, we measured stride length. Mice injected bilaterally with adenoviral virus at 10 wk of age were analyzed after 8 wk of injection. Mice were allowed to walk across a paper-lined chamber and into an enclosed box. After one practice run, tracings for front and rear footprints for each mouse were measured. Measurements were averaged and the data were presented as stride length in millimeters. To measure RotaRod performance, mice were trained for 5 min on three separate days on a RotaRod device (Rotamex 4/8; Columbus Instruments) at 5 rpm and tested at speeds of 4–40 rpm over a 5-min period. Latency to fall was recorded. Mice were allowed 10–20 min to recover between trials. Survival and body weight of mice were also monitored. Uninjected WT mice, $n = 11$; N171-82Q mice injected with adenoviral scFv-EM48, $n = 10$; N171-82Q mice injected with adenoviral vector control, $n = 9$; uninjected HD-N171-82Q mice, $n = 9$.

Dot blot analysis

A Hybond-P membrane (GE Healthcare) was rinsed in methanol and soaked in PBS. 2 µl of peptide solution in PBS were spotted on the x axis, with different dilutions (0, 1, 5, 25, 50, and 100 µM) on the y axis. The membrane was dried and blocked sequentially in 3% BSA and 5% milk in PBS for 1 h and then incubated overnight with mEM48 antibody at 4°C. The membrane was then rinsed with 5% milk/PBS three times and incubated with peroxidase-conjugated anti-mouse secondary antibody (Jackson ImmunoResearch Laboratories) at a 1:10,000 dilution in 5% milk/PBS for 1 h. The membrane was developed using ECL Plus reagents (GE Healthcare).

Protein binding assays and fractionation

We performed immunoprecipitation of transfected HEK293 and infected PC12 cells using the same method described previously (McGuire et al., 2006).

For peptide-blocking assays, the synthetic peptides (10–100 μM) were added to cell lysates before immunoprecipitation. Transfected scFv-EM48 was precipitated by mouse antibody to the HA epitope (12CA5) in PBS containing 0.2% Triton X-100 and protease inhibitor cocktail (Sigma-Aldrich). The precipitates were then analyzed by Western blotting with antibodies 12CA5 for the intrabody and rabbit EM48 or mEM48 for htt. PC12 cells were infected with adenoviral GFP-htt-130Q (Shin et al., 2005) and scFv-EM48. After 2 d, the infected cells were permeabilized in buffer (0.3% Triton X-100 in PBS containing protease inhibitors). Cytoplasmic proteins from permeabilized cells were centrifuged at 4,000 *g* for 10 min to be separated from nuclear materials and unbroken cells. Supernatant was then centrifuged at 16,000 *g* for 20 min. The cytoplasmic soluble and nonsoluble (pellet) proteins were collected for Western blot analysis. Pellets were also solubilized and immunoprecipitated by the anti-htt antibody EM48. The blots were probed with antibodies to htt, the HA epitope, tubulin, or ubiquitin.

For isolating synaptosomal fractions, striatum from N171-82Q mice that had been injected with either adenoviral vector or scFv-EM48 was dissected and homogenized in homogenizing buffer (0.3 g/ml in 225 mM mannitol, 75 mM sucrose, 10 mM MOPS, 1 mM EGTA, and 1:1,000 protease inhibitor cocktail, pH 7.2.) at 4°C using a glass homogenizer (Teflon; DuPont). 50 μl of the homogenate was served as total cell lysate. The remaining homogenate was centrifuged at 1,300 *g* for 5 min to yield the crude nuclear pellet (P1). The supernatant (S1) was transferred to a new tube and centrifuged at 13,000 *g* for 15 min, resulting in the cytosolic fraction (S2). The resulting pellet (P2) was resuspended in 15% Percoll in homogenizing buffer and carefully layered over a 26 and 40% discontinuous Percoll gradient in ultracentrifuge tubes. The gradient was centrifuged at 44,500 *g* at 4°C for 25 min. The synaptosomal layer (at the interface of 15 and 26% Percoll layers) was removed, washed with homogenizing buffer, and resuspended in RIPA buffer (50 mM Tris, pH 8.0, 150 mM NaCl, 1 mM EDTA, pH 8.0, 1 mM EGTA, pH 8.0, 0.1% SDS, 0.5% deoxycholate, and 1% Triton X-100). Crude nuclei (P1) were washed once each with buffer A (250 mM sucrose, 25 mM KCl, 5 mM MgCl2, 10 mM Hepes, and 0.6% NP-40) and buffer B (250 mM sucrose, 10 mM KCl, 10 mM MgCl2, and 10 mM Hepes), then resuspended in RIPA buffer. All fractions were assayed for protein amount using a detergent-compatible protein assay kit (Bio-Rad Laboratories). 30 μg of proteins from whole cell lysates and cytosolic, synaptosomal, and nuclear fractions were subjected to Western blotting.

Pulse-chase experiment

PC12 cells on 6-well tissue culture plates were infected with adenoviral GFP-htt-130Q and scFv-EM48 and cultured for 48 h. Metabolic labeling was performed by starving the cells in cysteine- and methionine-free DME (Invitrogen) supplemented with 5% fetal bovine serum for 1 h. Cells were pulse-labeled in the same medium containing 200 μCi/ml [^{35}S]methionine (GE Healthcare) for 40 min. Cells were subsequently washed twice and incubated (chased) in DME supplemented with 10% fetal bovine serum containing 2 mM methionine and cysteine for various amounts of time, collected by washing twice in ice-cold PBS, and lysed in 1 ml RIPA lysis buffer (50 mM Tris, pH 8.0, 150 mM NaCl, 1mM EDTA, 1mM EGTA, 0.1% SDS, 0.5% deoxycholate, and 1% Triton X-100) supplemented with protease inhibitors. The soluble lysate was precleared for 1 h with protein A–Sepharose at 4°C. The precleared lysate was immunoprecipitated with mEM48 antibody coupled to protein A–Sepharose for 6 h at 4°C. The precipitates were subjected to gel electrophoresis. The gel was fixed for 1 h in 10% acetic acid and 30% methanol and then impregnated in autoradiography enhancer (EN^{3}HANCE; PerkinElmer) for 1 h with gentle shaking. The gel was dried and exposed to an autoradiograph film (GE Healthcare) overnight.

Statistical analysis

Statistical significance ($P < 0.05$) was assessed using the Student's *t* test whenever two groups were compared. When analyzing multiple groups, we used analysis of variance with Scheffé's post hoc test to determine statistical significance. Data are presented as mean ± SEM. Calculations were performed with SigmaPlot 4.11 (System Software, Inc.) and GraphPad Prism software (GraphPad Software, Inc.).

Online supplemental material

Fig. S1 shows immunostaining of mutant htt by antibodies to different epitopes. Fig. S2 shows coexpression of scFV-EM48 with mutant ataxin-1 or ataxin-7. Fig. S3 shows the protective effect of scFM-EM48 in cultured primary neurons. Fig. S4 shows expression of adenoviral scFv-EM48. Fig. S5 shows coexpression of mutant htt (1–208 aa with 130Q) with the control intrabody NAC32-myc in HEK293 cells. Online supplemental material is available at http://www.jcb.org/cgi/content/full/jcb.200710158/DC1.

We thank P. Patterson and A. Khoshnan for their advice on the cloning of scFv; Z.H. Fang, G.Q. Sheng, J. Shin, A. Orr, and C. Clarke for technical assistance; H.T. Orr and A.R. La Spada for ataxin-1 and ataxin-7 plasmids; A. Messer for the NAC32-myc plasmid; M.R. Hayden for brain tissue samples from HD YAC128 mice; and M. Friedman and C. Strauss for critical reading of the manuscript.

This work was supported by the High Q Foundation and grants from the National Institutes of Health (NS052806, NS41669, AG19206, NS045016, and NS36232).

Submitted: 23 October 2007
Accepted: 30 April 2008

References

Arrasate, M., S. Mitra, E.S. Schweitzer, M.R. Segal, and S. Finkbeiner. 2004. Inclusion body formation reduces levels of mutant huntingtin and the risk of neuronal death. *Nature.* 431:805–810.

Benn, C.L., C. Landles, H. Li, A.D. Strand, B. Woodman, K. Sathasivam, S.H. Li, S. Ghazi-Noori, E. Hockly, S.M. Faruque, et al. 2005. Contribution of nuclear and extranuclear polyQ to neurological phenotypes in mouse models of Huntington's disease. *Hum. Mol. Genet.* 14:3065–3078.

Butler, R., and G.P. Bates. 2006. Histone deacetylase inhibitors as therapeutics for polyglutamine disorders. *Nat. Rev. Neurosci.* 7:784–796.

Chang, D.T., G.L. Rintoul, S. Pandipati, and I.J. Reynolds. 2006. Mutant huntingtin aggregates impair mitochondrial movement and trafficking in cortical neurons. *Neurobiol. Dis.* 22:388–400.

Colby, D.W., Y. Chu, J.P. Cassady, M. Duennwald, H. Zazulak, J.M. Webster, A. Messer, S. Lindquist, V.M. Ingram, and K.D. Wittrup. 2004. Potent inhibition of huntingtin aggregation and cytotoxicity by a disulfide bond-free single-domain intracellular antibody. *Proc. Natl. Acad. Sci. USA.* 101:17616–17621.

Cornett, J., F. Cao, C.E. Wang, C.A. Ross, G.P. Bates, S.H. Li, and X.J. Li. 2005. Polyglutamine expansion of huntingtin impairs its nuclear export. *Nat. Genet.* 37:198–204.

Davies, S.W., M. Turmaine, B.A. Cozens, M. DiFiglia, A.H. Sharp, C.A. Ross, E. Scherzinger, E.E. Wanker, L. Mangiarini, and G.P. Bates. 1997. Formation of neuronal intranuclear inclusions underlies the neurological dysfunction in mice transgenic for the HD mutation. *Cell.* 90:537–548.

DiFiglia, M., E. Sapp, K.O. Chase, S.W. Davies, G.P. Bates, J.P. Vonsattel, and N. Aronin. 1997. Aggregation of huntingtin in neuronal intranuclear inclusions and dystrophic neurites in brain. *Science.* 277:1990–1993.

Dorai, H., J.E. McCartney, R.M. Hudziak, M.S. Tai, A.A. Laminet, L.L. Houston, J.S. Huston, and H. Oppermann. 1994. Mammalian cell expression of single-chain Fv (sFv) antibody proteins and their C-terminal fusions with interleukin-2 and other effector domains. *Biotechnology (NY).* 12:890–897.

Dragatsis, I., M.S. Levine, and S. Zeitlin. 2000. Inactivation of Hdh in the brain and testis results in progressive neurodegeneration and sterility in mice. *Nat. Genet.* 26:300–306.

Ellerby, L.M., and H.T. Orr. 2006. Neurodegenerative disease: cut to the chase. *Nature.* 442:641–642.

Gatchel, J.R., and H.Y. Zoghbi. 2005. Diseases of unstable repeat expansion: mechanisms and common principles. *Nat. Rev. Genet.* 6:743–755.

Gauthier, L.R., B.C. Charrin, M. Borrell-Pages, J.P. Dompierre, H. Rangone, F.P. Cordelieres, J. De Mey, M.E. MacDonald, V. Lessmann, S. Humbert, and F. Saudou. 2004. Huntingtin controls neurotrophic support and survival of neurons by enhancing BDNF vesicular transport along microtubules. *Cell.* 118:127–138.

Graham, R.K., Y. Deng, E.J. Slow, B. Haigh, N. Bissada, G. Lu, J. Pearson, J. Shehadeh, L. Bertram, Z. Murphy, et al. 2006. Cleavage at the caspase-6 site is required for neuronal dysfunction and degeneration due to mutant huntingtin. *Cell.* 125:1179–1191.

Gunawardena, S., L.S. Her, R.G. Brusch, R.A. Laymon, I.R. Niesman, B. Gordesky-Gold, L. Sintasath, N.M. Bonini, and L.S. Goldstein. 2003. Disruption of axonal transport by loss of huntingtin or expression of pathogenic polyQ proteins in *Drosophila*. *Neuron.* 40:25–40.

Gutekunst, C.A., S.H. Li, H. Yi, J.S. Mulroy, S. Kuemmerle, R. Jones, D. Rye, R.J. Ferrante, S.M. Hersch, and X.J. Li. 1999. Nuclear and neuropil aggregates in Huntington's disease: relationship to neuropathology. *J. Neurosci.* 19:2522–2534.

Harper, S.Q., P.D. Staber, X. He, S.L. Eliason, I.H. Martins, Q. Mao, L. Yang, R.M. Kotin, H.L. Paulson, and B.L. Davidson. 2005. RNA interference improves motor and neuropathological abnormalities in a Huntington's disease mouse model. *Proc. Natl. Acad. Sci. USA.* 102:5820–5825.

Hudson, P.J., and C. Souriau. 2003. Engineered antibodies. *Nat. Med.* 9:129–134.

Jackson, W.S., S.J. Tallaksen-Greene, R.L. Albin, and P.J. Detloff. 2003. Nucleocytoplasmic transport signals affect the age at onset of abnormalities in knock-in mice expressing polyglutamine within an ectopic protein context. *Hum. Mol. Genet.* 12:1621–1629.

Khoshnan, A., J. Ko, and P.H. Patterson. 2002. Effects of intracellular expression of anti-huntingtin antibodies of various specificities on mutant huntingtin aggregation and toxicity. *Proc. Natl. Acad. Sci. USA.* 99:1002–1007.

Lecerf, J.M., T.L. Shirley, Q. Zhu, A. Kazantsev, P. Amersdorfer, D.E. Housman, A. Messer, and J.S. Huston. 2001. Human single-chain Fv intrabodies counteract in situ huntingtin aggregation in cellular models of Huntington's disease. *Proc. Natl. Acad. Sci. USA.* 98:4764–4769.

Lee, W.C., M. Yoshihara, and J.T. Littleton. 2004. Cytoplasmic aggregates trap polyglutamine-containing proteins and block axonal transport in a *Drosophila* model of Huntington's disease. *Proc. Natl. Acad. Sci. USA.* 101:3224–3229.

Li, H., S.H. Li, A.L. Cheng, L. Mangiarini, G.P. Bates, and X.J. Li. 1999. Ultrastructural localization and progressive formation of neuropil aggregates in Huntington's disease transgenic mice. *Hum. Mol. Genet.* 8:1227–1236.

Li, H., S.H. Li, H. Johnston, P.F. Shelbourne, and X.J. Li. 2000. Amino-terminal fragments of mutant huntingtin show selective accumulation in striatal neurons and synaptic toxicity. *Nat. Genet.* 25:385–389.

Li, H., S.H. Li, Z.X. Yu, P. Shelbourne, and X.J. Li. 2001. Huntingtin aggregate-associated axonal degeneration is an early pathological event in Huntington's disease mice. *J. Neurosci.* 21:8473–8481.

Li, S.H., and X.J. Li. 2004. Huntingtin-protein interactions and the pathogenesis of Huntington's disease. *Trends Genet.* 20:146–154.

Lobato, M.N., and T.H. Rabbitts. 2004. Intracellular antibodies as specific reagents for functional ablation: future therapeutic molecules. *Curr. Mol. Med.* 4:519–528.

Lunkes, A., K.S. Lindenberg, L. Ben-Haiem, C. Weber, D. Devys, G.B. Landwehrmeyer, J.L. Mandel, and Y. Trottier. 2002. Proteases acting on mutant huntingtin generate cleaved products that differentially build up cytoplasmic and nuclear inclusions. *Mol. Cell.* 10:259–269.

Lynch, S.M., C. Zhou, and A. Messer. 2008. An scFv intrabody against the non-amyloid component of alpha-synuclein reduces intracellular aggregation and toxicity. *J. Mol. Biol.* 377:136–147.

McGuire, J.R., J. Rong, S.H. Li, and X.J. Li. 2006. Interaction of Huntingtin-associated protein-1 with kinesin light chain: implications in intracellular trafficking in neurons. *J. Biol. Chem.* 281:3552–3559.

Miller, T.W., C. Zhou, S. Gines, M.E. MacDonald, N.D. Mazarakis, G.P. Bates, J.S. Huston, and A. Messer. 2005. A human single-chain Fv intrabody preferentially targets amino-terminal Huntingtin's fragments in striatal models of Huntington's disease. *Neurobiol. Dis.* 19:47–56.

Parker, J.A., J.B. Connolly, C. Wellington, M. Hayden, J. Dausset, and C. Neri. 2001. Expanded polyglutamines in *Caenorhabditis elegans* cause axonal abnormalities and severe dysfunction of PLM mechanosensory neurons without cell death. *Proc. Natl. Acad. Sci. USA.* 98:13318–13323.

Piccioni, F., P. Pinton, S. Simeoni, P. Pozzi, U. Fascio, G. Vismara, L. Martini, R. Rizzuto, and A. Poletti. 2002. Androgen receptor with elongated polyglutamine tract forms aggregates that alter axonal trafficking and mitochondrial distribution in motor neuronal processes. *FASEB J.* 16:1418–1420.

Saudou, F., S. Finkbeiner, D. Devys, and M.E. Greenberg. 1998. Huntingtin acts in the nucleus to induce apoptosis but death does not correlate with the formation of intranuclear inclusions. *Cell.* 95:55–66.

Schilling, G., M.W. Becher, A.H. Sharp, H.A. Jinnah, K. Duan, J.A. Kotzuk, H.H. Slunt, T. Ratovitski, J.K. Cooper, N.A. Jenkins, et al. 1999. Intranuclear inclusions and neuritic aggregates in transgenic mice expressing a mutant N-terminal fragment of huntingtin. *Hum. Mol. Genet.* 8:397–407. (published erratum appears in *Hum. Mol. Genet.* 1999. 8:943).

Shin, J.Y., Z.H. Fang, Z.X. Yu, C.E. Wang, S.H. Li, and X.J. Li. 2005. Expression of mutant huntingtin in glial cells contributes to neuronal excitotoxicity. *J. Cell Biol.* 171:1001–1012.

Sugars, K.L., and D.C. Rubinsztein. 2003. Transcriptional abnormalities in Huntington disease. *Trends Genet.* 19:233–238.

Szebenyi, G., G.A. Morfini, A. Babcock, M. Gould, K. Selkoe, D.L. Stenoien, M. Young, P.W. Faber, M.E. MacDonald, M.J. McPhaul, and S.T. Brady. 2003. Neuropathogenic forms of huntingtin and androgen receptor inhibit fast axonal transport. *Neuron.* 40:41–52.

Tallaksen-Greene, S.J., A.B. Crouse, J.M. Hunter, P.J. Detloff, and R.L. Albin. 2005. Neuronal intranuclear inclusions and neuropil aggregates in HdhCAG(150) knockin mice. *Neuroscience.* 131:843–852.

Toietta, G., L. Pastore, V. Cerullo, M. Finegold, A.L. Beaudet, and B. Lee. 2002. Generation of helper-dependent adenoviral vectors by homologous recombination. *Mol. Ther.* 5:204–210.

Toietta, G., V.P. Mane, W.S. Norona, M.J. Finegold, P. Ng, A.F. McDonagh, A.L. Beaudet, and B. Lee. 2005. Lifelong elimination of hyperbilirubinemia in the Gunn rat with a single injection of helper-dependent adenoviral vector. *Proc. Natl. Acad. Sci. USA.* 102:3930–3935.

Trushina, E., R.B. Dyer, J.D. Badger II, D. Ure, L. Eide, D.D. Tran, B.T. Vrieze, V. Legendre-Guillemin, P.S. McPherson, B.S. Mandavilli, et al. 2004. Mutant huntingtin impairs axonal trafficking in mammalian neurons in vivo and in vitro. *Mol. Cell. Biol.* 24:8195–8209.

Wellington, C.L., L.M. Ellerby, C.A. Gutekunst, D. Rogers, S. Warby, R.K. Graham, O. Loubser, J. van Raamsdonk, R. Singaraja, Y.Z. Yang, et al. 2002. Caspase cleavage of mutant huntingtin precedes neurodegeneration in Huntington's disease. *J. Neurosci.* 22:7862–7872.

White, J.K., W. Auerbach, M.P. Duyao, J.P. Vonsattel, J.F. Gusella, A.L. Joyner, and M.E. MacDonald. 1997. Huntingtin is required for neurogenesis and is not impaired by the Huntington's disease CAG expansion. *Nat. Genet.* 17:404–410.

Wolfgang, W.J., T.W. Miller, J.M. Webster, J.S. Huston, L.M. Thompson, J.L. Marsh, and A. Messer. 2005. Suppression of Huntington's disease pathology in *Drosophila* by human single-chain Fv antibodies. *Proc. Natl. Acad. Sci. USA.* 102:11563–11568.

Yamamoto, A., J.J. Lucas, and R. Hen. 2000. Reversal of neuropathology and motor dysfunction in a conditional model of Huntington's disease. *Cell.* 101:57–66.

Yu, Z.X., S.H. Li, J. Evans, A. Pillarisetti, H. Li, and X.J. Li. 2003. Mutant huntingtin causes context-dependent neurodegeneration in mice with Huntington's disease. *J. Neurosci.* 23:2193–2202.

Zhou, H., F. Cao, Z. Wang, Z.X. Yu, H.P. Nguyen, J. Evans, S.H. Li, and X.J. Li. 2003. Huntingtin forms toxic NH_2-terminal fragment complexes that are promoted by the age-dependent decrease in proteasome activity. *J. Cell Biol.* 163:109–118.

Zoghbi, H.Y., and H.T. Orr. 2000. Glutamine repeats and neurodegeneration. *Annu. Rev. Neurosci.* 23:217–247.